Neuroscience 288 (2015) 135–144

THE ENDOCANNABINOID SYSTEM WITHIN THE DORSAL LATERAL GENICULATE NUCLEUS OF THE VERVET MONKEY

P. JAVADI, [a] **J. BOUSKILA,** [a,b] **J.-F. BOUCHARD** [a] **AND M. PTITO** [a,c,d*]

[a] *School of Optometry, University of Montreal, Montreal, QC, Canada*

[b] *Biomedical Sciences, Faculty of Medicine, University of Montreal, Montreal, QC, Canada*

[c] *BRAINlab, Department of Neuroscience and Pharmacology, University of Copenhagen, Copenhagen, Denmark*

[d] *Laboratory of Neuropsychiatry, Psychiatric Centre Copenhagen and Department of Neuroscience and Pharmacology, University of Copenhagen, DK-2100 Copenhagen, Denmark*

Abstract—The endocannabinoid system mainly consists of cannabinoid receptors type 1 (CB1R) and type 2 (CB2R), their endogenous ligands termed endocannabinoids (eCBs), and the enzymes responsible for the synthesis and degradation of eCBs. These cannabinoid receptors have been well characterized in rodent and monkey retinae. Here, we investigated the expression and localization of the eCB system beyond the retina, namely the first thalamic relay, the dorsal lateral geniculate nucleus (dLGN), of vervet monkeys using immunohistochemistry methods. Our results show that CB1R is expressed throughout the dLGN with more prominent labeling in the magnocellular layers. The same pattern is observed for the degradation enzyme, fatty acid amide hydrolase (FAAH). However, the synthesizing enzyme N-acyl-phosphatidylethanolamine phospholipase D (NAPE-PLD) is expressed homogenously throughout the dLGN with no preference for any of the layers. These proteins are weakly expressed in the koniocellular layers. These results suggest that the presence of the eCB system throughout the layers of the dLGN may represent a novel site of neuromodulatory action in normal vision. The larger amount of CB1R in the dLGN magnocellular layers may explain some of the behavioral effects of cannabinoids associated with the integrity of the dorsal visual pathway that plays a role in visual-spatial localization and motion perception.

Key words: CB1R, FAAH, NAPE-PLD, dLGN, monkey, cannabinoid receptors.

INTRODUCTION

The physiological and psychological effects of phytocannabinoids, the active components of the cannabis plant, can be detected almost everywhere in the body due to their actions on specific receptors: mainly the cannabinoid receptors type 1 (CB1R) and type 2 (CB2R). Cannabinoid receptors are membrane receptors principally coupled to inhibitory G-proteins that modulate the release of neurotransmitters (Piomelli, 2003; Gómez-Ruiz et al., 2007). They mediate biological functions not only via the exogenous cannabinoids, but also via eCBs such as N-arachidonoylethanolamide (anandamide or AEA) and 2-arachidonoylglycerol (2-AG). Unlike the classical neurotransmitters, eCBs are synthesized "on demand" by catalyzing the release of N-acylethanolamines (NAEs) from N-acyl-phosphatidylethanolamine (NAPE) by specific enzyme, like N-acyl-phosphatidylethanolamine phospholipase D (NAPE-PLD) or from arachidonic acid via diacylglycerol lipase enzyme (DAGL). The eCBs are not accumulated into synaptic vesicles and are rather degraded rapidly by specific enzymes like fatty acid amid hydrolase (FAAH) and monoglycerol lipase (MAGL) (for review, see Deutsch and Chin, 1993).

The localization and function of the molecular components of the eCB system in the central nervous system have been the subject of recent research. In fact, the role of the eCB system in learning, memory, neuroprotection and visual processing is essentially due to the modulation of neurotransmitter release by the presynaptic location of CB1R (Di Marzo et al., 1998; Straiker et al., 1999a). CB1R expression is found in the hippocampus, prefrontal cortex, cerebellum and basal ganglia of rodents (Herkenham et al., 1991) and primates (Eggan and Lewis, 2007). It is expressed in glutamatergic and GABAergic neurons throughout the central and peripheral nervous systems (Egertová and Elphick, 2000). In the visual system, CB1R and FAAH have been localized in cone photoreceptors, horizontal, amacrine, bipolar, and retinal ganglion cells in the central and peripheral retina of vervet monkeys (Bouskila et al., 2012). CB1R is also found in the human retina (Straiker et al., 1999b).

*Correspondence to: M. Ptito, School of Optometry, University of Montreal, Room 260-7, 3744 Jean-Brillant Street, Montreal, QC H3T 1P1, Canada. Tel: +1-514-343-6052.
E-mail address: maurice.ptito@umontreal.ca (M. Ptito).

Abbreviations: AEA, anandamide; CB1R, cannabinoid receptor CB1; DAB, 3,3′-diaminobenzidine; DAGL, diacylglycerol lipase enzyme; dLGN, dorsal lateral geniculate nucleus; eCB, endocannabinoid; ERG, electroretinogram; FAAH, fatty acid amide hydrolase; GABA, GABAergic cell; GFAP, glial fibrillary acidic protein; IR, immunoreactivity; MAGL, monoglycerol lipase; MT, middle temporal; MST, medial superior temporal; NAE, N-acylethanolamines; NAPE, N-acyl-phosphatidylethanolamine; NAPE-PLD, N-acyl-phosphatidylethanolamine phospholipase D; NDS, normal donkey serum; PBS, phosphate-buffered saline; SEM, standard error of the mean; VGLUT1, vesicular glutamate transporter 1; 2-AG, 2-arachidonoylglycerol.

http://dx.doi.org/10.1016/j.neuroscience.2014.12.029
0306-4522/

Earlier studies reported that cannabis could affect several visual functions, such as photosensitivity (Adams et al., 1978), visual acuity (Moskowitz et al., 1972; Adams and Brown, 1975), color vision (Dawson et al., 1977), ocular tracking (Flom et al., 1976), binocular depth inversion, and stereoscopic vision (Emrich et al., 1991; Leweke et al., 1999; Semple et al., 2003). Some case studies later claimed other visual effects of cannabis such as visual distortions, altered perception of distance, illusions of movement in stationary and moving objects, color intensification of objects, dimensional distortion and blending of patterns and objects (Levi and Miller, 1990; Lerner et al., 2011). Given the localization of CB1R in the central retina, from cones to ganglion cells, it is reasonable to assume its implication in these visual manifestations.

In homogenates of rodent thalamus, high levels of AEA (Felder et al., 1996) and FAAH (Egertová et al., 2003), as well as an elevated cannabinoid receptor/G-protein amplification ratio (Breivogel et al., 1997) have been found. Also, using immunohistochemistry, moderate to low levels of CB1R expressions have been found in the thalamus of rats (Egertová et al., 1998; Tsou et al., 1998; Moldrich and Wenger, 2000), non-human primates (Ong and Mackie, 1999) and humans (Glass et al., 1997) without focusing on dorsal lateral geniculate nucleus (dLGN). However, there is no study, to our knowledge, that has thoroughly studied the expression of the eCB system in this retino-recipient primary thalamic relay of the primate. Similar to apes and humans, the dLGN of vervet monkeys consists of six layers. The first two ventral layers, the magnocellular layers, receive input from large ganglion cells (rod signals) and are necessary for the perception of movement, depth and small difference in brightness. The four dorsal layers, parvocellular layers, receive input from small ganglion cells of the retina (cone signals) and play a role in color and form perception. These layers are well separated by an inter-laminar zone called koniocellular layers that contribute to short-wavelength "blue" cones (Xu et al., 2001). Given the expression and localization of CB1R in the retinal mosaic, we expect to find this receptor in the optic nerve and the dLGN layers.

EXPERIMENTAL PROCEDURES

Animals

Monkey tissues were obtained from four adult vervet monkeys (*Chlorocebus sabaeus*). The monkeys were part of Dr. Ptito's and Dr. Palmour's research project that was approved by McGill University Animal Care and Use Committee. The animals were born and raised under an enriched natural environment in the laboratories of the Behavioral Sciences Foundation (St-Kitts, West Indies), a facility recognized by the Canadian Council on Animal Care (CCAC). The experimental protocol was reviewed and approved by the local Animal Care and Use Committee (University of Montreal) and the Institutional Review Board of the Behavioral Science Foundation.

Tissue preparation

Each animal was sedated with ketamine hydrochloride (10 mg/kg, i.m.) and euthanized by an overdose of intravenously administered sodium pentobarbital (25 mg/kg), followed by transcardial perfusion of 0.1 M phosphate-buffered saline (PBS) (pH 7.4). The brains were then removed, blocked and flash-frozen in an isopentane bath cooled in a dry ice chamber and maintained at −80 °C. The blocks were cut along the coronal plane in 20-μm sections at −18 °C on a Leica CM3050S cryostat and mounted onto gelatinized subbed glass slides. The slide-mounted tissue sections were stored at −80 °C until further histological processing.

Immunohistochemistry (DAB)

At least one slide-mounted 20-μm fresh-frozen tissue section per animal was selected from A6 to A9, at a level where the lamination of the dLGN is the clearest and thawed at room temperature. A hydrophobic barrier was created surrounding the slides, using PAP pen (Vector, Burlingame, CA, USA) to keep staining reagents localized on the tissue section. Sections were fixed with 70% ethanol solution for 15 min, followed by two 5-min rinses with 0.1 M Tris buffer, pH 7.4/0.03% Triton X-100. To block the endogenous peroxidase activity, sections were washed with 0.3% hydrogen peroxide in PBS for 15 min. Following three times 5-min PBS-triton rinse, sections were blocked for 60 min with a solution of 10% normal donkey serum (NDS) and 0.1 M Tris buffer/0.5% Triton. Each section was incubated overnight at room temperature with primary antibodies (Table 1) diluted in the blocking solution. The next day, sections underwent three 10-min PBS-triton washes, followed by incubation in a secondary antibody solution (biotinylated donkey anti-rabbit antibody diluted 1:200 in blocking solution) for 2 h. After three consecutive 10-min washes with PBS-triton, the sections were incubated for 1 h in an avidin–biotin-conjugated horseradish peroxidase (Vectastain ABC kit, Burlingame, CA, USA) solution (1:500). Following three subsequent 10-min washes in PBS-triton, the sections were treated with a 3,3′-diaminobenzidine (DAB) substrate. After rinsing in PBS-triton three times for 5 min each, sections underwent dehydration in graded ethanol steps, cleared in xylene, and cover-slipped with Permount mounting media (Fisher Scientific; Pittsburgh, PA, USA). Sections were examined on a Leica DMRB under bright field illumination.

Immunofluorescence

Double and triple labeling of the brain tissues were performed according to previously published methods on the vervet monkey retina (Bouskila et al., 2012; Bouskila et al., 2013a,b). Briefly, sections were post-fixed for 15 min in 70% ethanol, rinsed two times for 5 min in 0.1 M Tris buffer, pH 7.4/0.03% Triton and blocked for 90 min in 10% NDS and 0.1 M Tris buffer/0.5% Triton. Sections were incubated overnight at room temperature

Table 1. Primary antibodies used in this study

Antibody	Immunogen	Source	Working dilution
CB1R	Fusion protein containing aa 1–77 of rat CB1R	Sigma, St. Louis, MO C1233, Rabbit polyclonal	H: 1:200
FAAH	Synthetic peptide aa 561–579 of rat FAAH	Cayman Chemical, Ann Arbor, MI, 101600, rabbit polyclonal	H: 1:200
NAPE-PLD	Synthetic peptide aa 159–172 of human NAPE-PLD	Cayman Chemical, Ann Arbor, MI, 10305, rabbit, polyclonal	H: 1:200
GFAP	Purified protein isolated from pig spinal cord	Sigma-Aldrich, St. Louis, MO, G3893, mouse, G-A-5, monoclonal	H: 1:200
VGLUT1	Fusion protein containing aa 456–560 of rat VGLUT1	Synaptic System, Goettingen, Germany,135 311, mouse, 317D5 monoclonal	H: 1:200
GABA	Fusion Protein coupling to BSA with glutaraldehyde	Millipore, MA, MAB316, Monoclonal	H: 1:200

with primary antibodies in blocking solution. The antibodies directed against molecular eCB components all raised in rabbit were used conjointly with a known cell marker: glial fibrillary acidic protein (GFAP) (astrocytes marker), vesicular glutamate transporter 1 (VGLUT1) (glutamatergic cell marker) and GABA (GABAergic cell marker) (Table 1). The next day, sections were washed for 10-min and two times for 5 min in 0.1 M Tris/0.03% Triton and incubated with biotinylated donkey anti-rabbit diluted 1:200 in blocking solution for 2 h for the eCB targets to amplify the signals. Sections were then incubated for another 2 h with streptavidin 647 in order to amplify the signal and alexa 555 or 488 secondary antibodies when necessary. Sections were cover-slipped with Fluoromount-G™ Mounting Medium (SouthernBiotech, Birmingham, AL, USA) after 3 × 10 min washes with 0.1 M Tris buffer. In the case of the GABA antibody, the sections had to be fixed in PFA 4% and glutaraldehyde 1%. The GABA signals were amplified with biotinylated donkey anti-mouse and the cannabinoid signals with donkey anti rabbit HRP and alexa fluor tyramide (Invitrogen, Eugene, Oregon).

Antibody characterization

The source and working dilution of all primary antibodies used in this study are summarized in Table 1. The antibodies with the exception of NAPE-PLD were successfully used in previous studies and were well characterized in the vervet monkey (Bouskila et al., 2012).

CB1R. The rabbit anti-CB1R (Calbiochem, Gibbstown, NJ, USA) was developed using a highly purified fusion protein with the first 77 amino acid residues of rat CB1R. According to the manufacturer's data sheet, it recognizes a major band of 60 kDa with also less intense bands of 23, 72, and 180 kDa. This antibody was shown to be specific using CB1R knockout mouse retinal tissue (Zabouri et al., 2011). It recognizes the CB1R (60 kDa) from many species, including the vervet monkey tissues (Bouskila et al., 2012).

GFAP. The mouse anti-glial fibrillary acidic protein (GFAP, Clone G-A-5, Sigma–Aldrich, St. Louis, MO, USA) was produced using purified GFAP isolated from the pig spinal cord. This antibody recognizes the GFAP protein of 50 kDa in Western blots (manufacturer's data sheet). GFAP stains cells with the morphology and distribution expected for astrocytes in monkey dLGN (Takahata et al., 2010).

FAAH. The rabbit anti-fatty acid amide hydrolase (FAAH, Cayman Chemical, Ann Arbor, MI, USA) was developed using a synthetic peptide from rat FAAH amino acids 561–579 (CLRFMREVEQLMTPQKQPS) conjugated to KLH. As expected, it recognizes a dense band at about 66 kDa and a very light one below 37 kDa. The specificity of this antibody has been demonstrated in rat (Suárez et al., 2008; Zabouri et al., 2011) and vervet monkey (Bouskila et al., 2012) tissues.

NAPE-PLD. The rabbit anti-N-acyl phosphatidylethanolamine-specific phospholipase D (NAPE-PLD, Cayman Chemical, Ann Arbor, MI, USA) was developed using a synthetic peptide from human NAPE-PLD amino acids 159–172 (YMGPKRFRRSPCTI). Its cross reactivity has been tested in many species, and it recognizes an intense band at 46 kDa on Western blot of the human cerebellum (manufacturer's data sheet).

NAPE-PLD blocking peptide. The NAPE-PLD blocking peptide containing the human NAPE-PLD amino acid sequence 159–172 (YMGPKRFRRSPCTI; Cayman Chemical, Ann Arbor, MI, USA) was used in the present study for Western blot analysis. The specificity of the NAPE-PLD antibody was tested by pre-incubation with the corresponding blocking peptide. For pre-adsorption, the primary antibody was diluted in PBS and incubated with a ratio 1:5 for 2 h at room temperature, with occasional inversion. Thereafter, the antibody-blocking peptide solution was added to the blot and subsequent Western blotting followed the protocol as described further.

VGLUT1. The mouse anti-vesicular glutamate transporter 1 (VGLUT1, Synaptic System, Goettingen, Germany) was raised against the aa 456–560 of the rat VGLUT1 protein. It is used as a glutamatergic neuron marker and its specificity has been verified in *vglut1* KO mouse tissue (Wojcik et al., 2004) as well as using the corresponding blocking peptide (Zhou et al., 2007).

GABA. The mouse anti-gamma aminobutyric acid antibody (GABA, Millipore, MA, USA) was synthesized coupling to BSA with glutaraldehyde. It is used as a marker of GABAergic neurons. Thus, for the GABA antibody, sections were fixed for 20 min in 1% glutaraldehyde, 4% PFA in PBS. The antibody has been frequently used in different animals, and its specificity has been verified in monkey (Jongen-Relo et al., 1999).

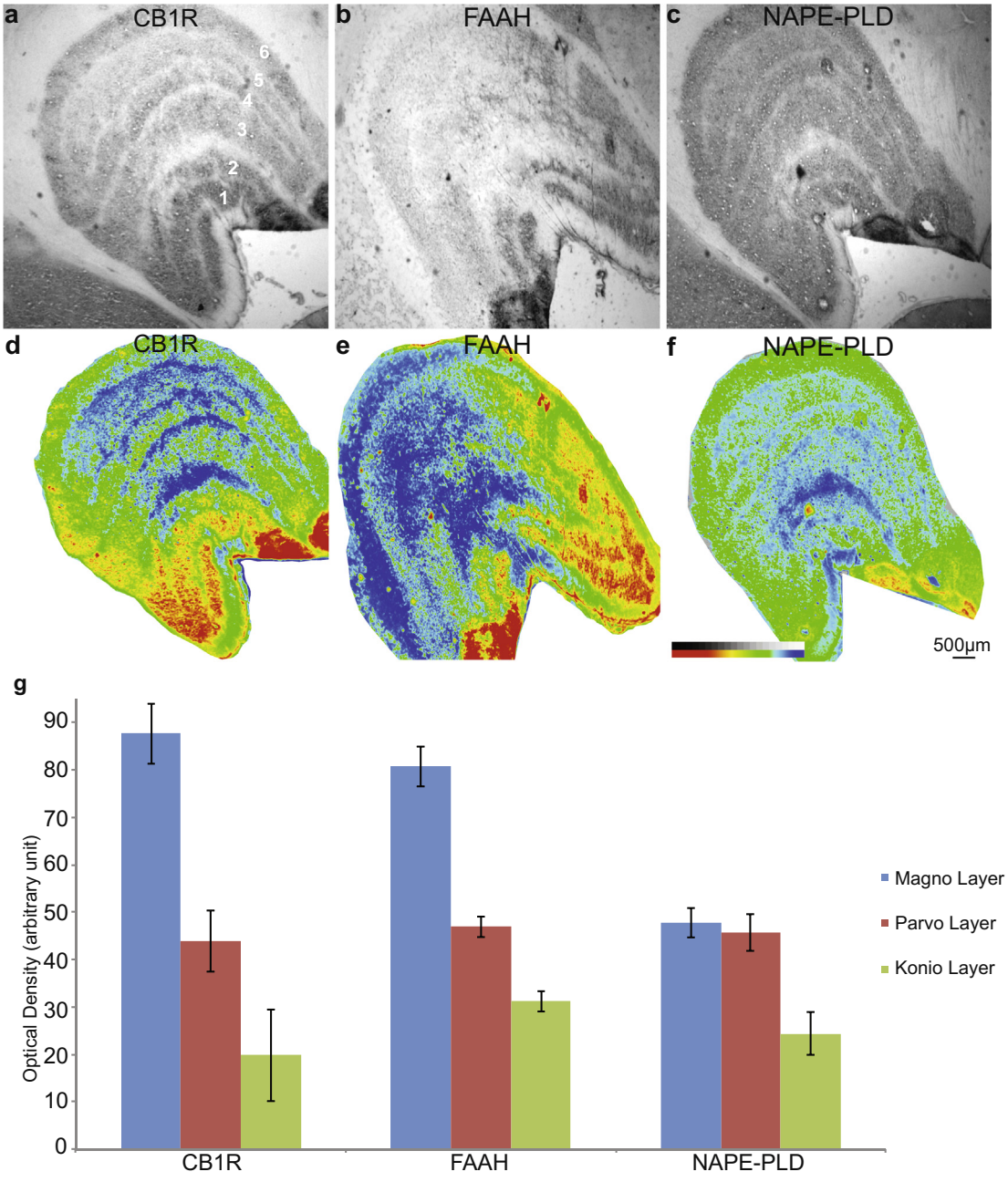

Fig. 1. Spatial distribution of CB1R, FAAH, and NAPE-PLD throughout the dLGN (a–c) of vervet monkeys. The RGB heat map was used to enhance the display of the abundance of the CB1R (d), FAAH (e) and NAPE-PLD (f) in the dLGN. The gray spectrum was distributed within the RGB spectral subdivision in which the maximum threshold gray values were expressed as red and the minimum as blue. CB1R is more expressed within the first two layers of dLGN. FAAH expression pattern is similar to CB1R. The NAPE-PLD expression is similarly distributed throughout the magno and parvo cellular layers. Scale bars = 500 µm. (g) Quantification of the mean contrast intensity of CB1R, FAAH and NAPE-PLD-IR in magno-, parvo- and koniocellular layer. The bars indicate the standard error. (For interpretation of the references to color in this figure legend, the reader is referred to the web version of this article.)

Microscopy

To detect the fluorescence signals, a Leica TCS SP2 confocal laser-scanning microscope (Leica Microsystems, Exton, PA, USA) with 40× (n.a. 1.25–0.75) and 100x (n.a. 1.40–0.7) objectives was used. Subsequently, images were acquired from the green and far-red channels on optical slices of less than 0.9 μm. Adobe Photoshop (CS5; Adobe Systems, San Jose, CA, USA) was used for all photomicrographic adjustments on size, color and shape before exporting them to Adobe InDesign (CS5; Adobe Systems), where the final figure layout was completed. For DAB staining, all photomicrographs were captured with a Leica DMR photomicroscope equipped with a Retiga 1300 video camera system (Q Imaging) using the QCapture software with a Leica 2.5× (n.a. 0.07) objective.

Quantification

In order to enhance the visualization of CB1R spatial distribution throughout the dLGN layers, photomicrographs demonstrating the entire structure were generated in an 8-bit gray scale. Using a MatLab code, the minimum and maximum thresholds of the gray values in the image were measured. The gray spectrum values were then eventually distributed within the RGB spectral subdivision in which the maximum threshold gray values were presented in red and the minimum in blue. Moreover, the average contrast intensity of each layer was calculated using the FIJI program (v. 1.48t, Wayn Rasband, NIH, USA). The program was calibrated using a calibration grid slide. The RGB images were inverted to 8-bit with a linear gray scaling from a minimum to a maximum pixel intensity (arbitrary value 0–255). The

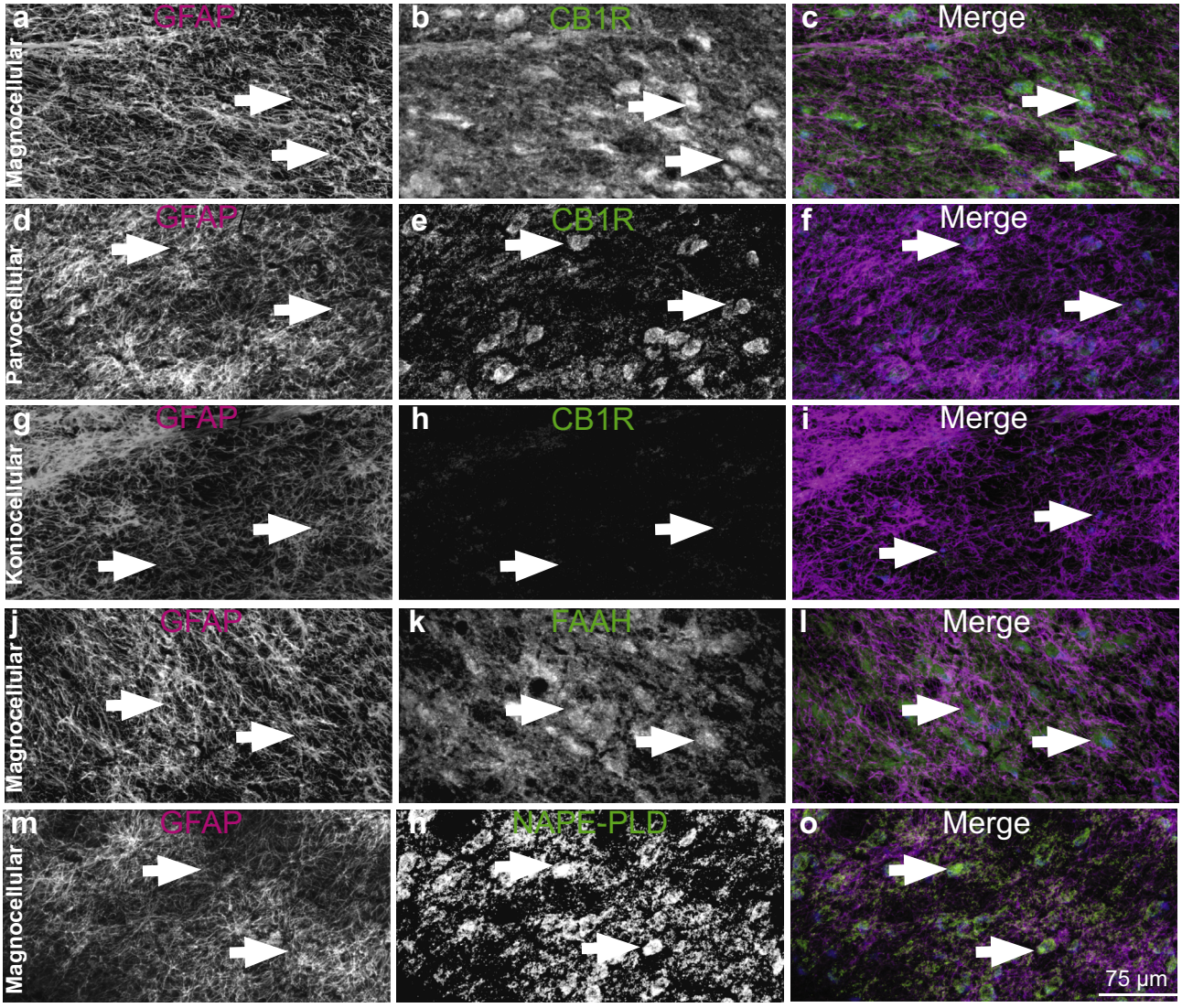

Fig. 2. Triple-label immunofluorescence of the CB1R (magenta) and GFAP (green) expression with nucleic acid stain Sytox (blue), respectively in magnocellular (a–c), parvocellular (d–f) and koniocellular layers (g–i). The absence of GFAP with FAAH (j–l) and NAPE-PLD (m–o) co-localizations in the magnocellular layers of the monkey dLGN are shown. Each immunostaining is presented alone in gray scale in the first two columns (1st column: GFAP and 2nd column: CB) following their merged image in the third column. Arrows point at GFAP cell bodies with no expression of CB. Scale bars = 75 μm. (For interpretation of the references to color in this figure legend, the reader is referred to the web version of this article.)

mean intensity of four sections (per condition) in their whole magno-, parvo- and koniocellular layers (±SEM) was reported after subtracting the average background intensity.

RESULTS

Spatial expression of the endocannabinoid system in dLGN

To examine the laminar expression of the endocannabinoid system profile in dLGN, tissues were labeled with specific antibodies against CB1R, FAAH, and NAPE-PLD. Their expression pattern in the brain was quantified using heatmap analysis. Immunolabeled sections for CB1R were found throughout the magnocellular and parvocellular layers of the dLGN with a higher intensity in the magnocellular layers (Fig. 1a, d, g). The koniocellular layers had the lowest expression of CB1R (Fig. 1a, d, g). Similar patterns of expression were observed for FAAH (Fig. 1b, e, g). NAPE-PLD was expressed homogenously with no preferences for the magnocellular or parvocellular layers. The koniocellular layers still showed very low expression of the synthesizing enzyme (Fig. 1c, f, g). A consistent staining pattern across all four monkeys dLGN was found. Interestingly, all these three proteins were also highly expressed in the optic nerve (data not shown).

CB1R, FAAH and NAPE-PLD are not present in LGN astrocytes

The double immunostaining was carried out with molecular markers to examine the eCB system expression at the cellular level. Cytosolic spread expression of CB1R is not co-localized with GFAP-positive glial cells (Fig. 2a–f). There is an apparent higher expression of CB1R in the magnocellular layers

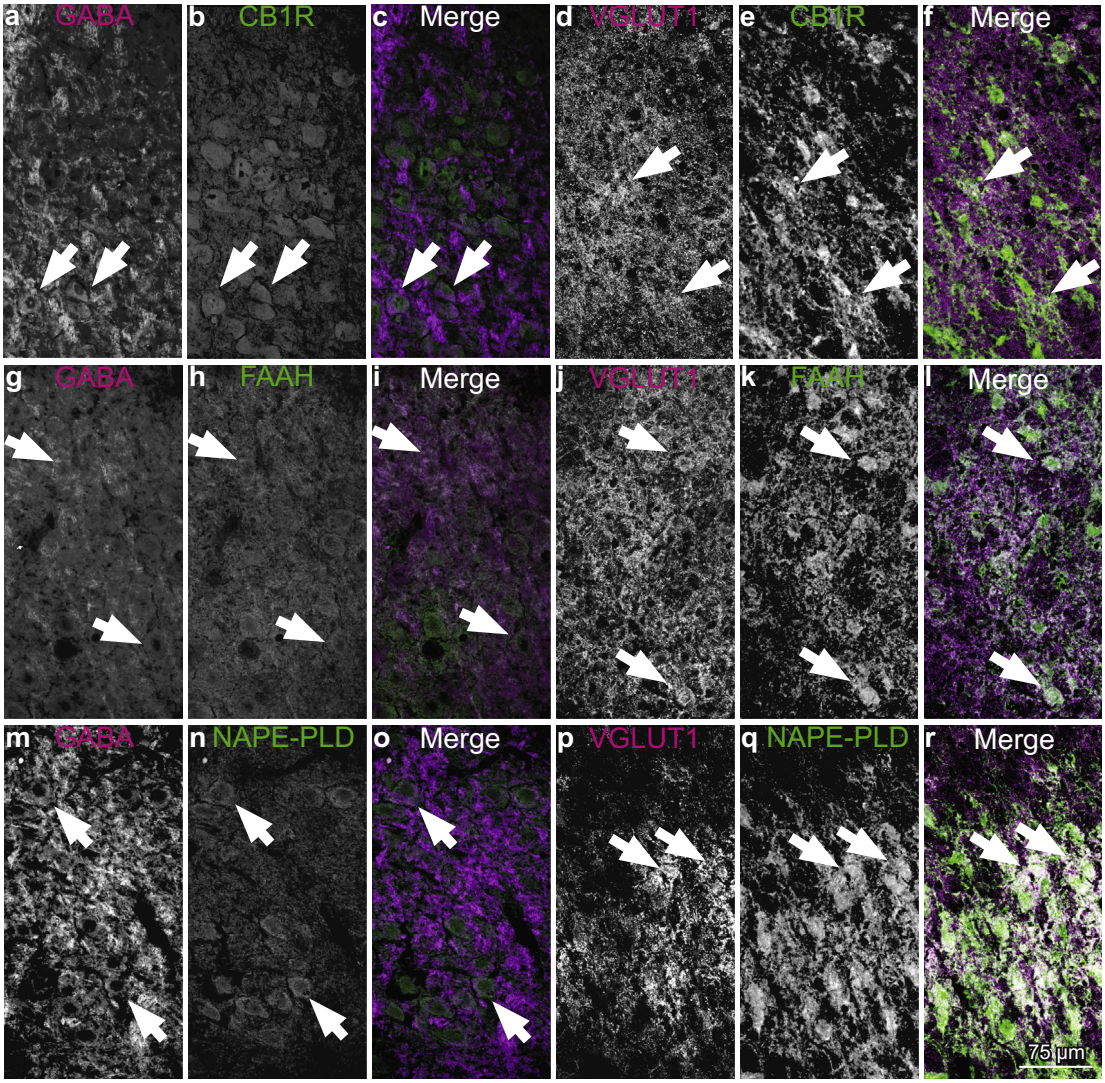

Fig. 3. Immunofluorescence labeling illustrating the co-localization of CB1R (a–f), FAAH (g–l) and NAPE-PLD (m–r) with GABAergic (three left columns) and glutamatergic (three right columns) neurons in the magnocellular layer 1 of the dLGN. Each immunostaining is presented alone in gray scale in the first two columns following their merged image in the third column. Arrows point to the co-localization of eCB components with GABA and VGLUT1. Scale bar = 75 µm.

(Fig. 2a–c) compared to the parvocellular layers (Fig. 2d–f). The very weak expression of this receptor in the koniocellular layers is also evident (Fig. 1g, h). Similarly, FAAH-IR is not detected in astrocytes of magnocellular layer (Fig. 2j–l).

In contrast to the difference in the pattern of expression of NAPE-PLD, the cellular expression of this synthesizing enzyme is similar to that of CB1R and FAAH. NAPE-PLD is also absent in astrocytes; however, it is abundant in the cytosol of the both magnocellular (Fig. 2m–o) and parvocellular (data not shown) dLGN neurons.

CB1R, FAAH and NAPE-PLD are expressed in glutamatergic and GABAergic neurons

As previously reported in the rat brain, CB1R is expressed in both GABAergic and glutamatergic cells (Egertová and Elphick, 2000). Our results validate the expression of CB1R within the GABAergic (Fig. 3a–c) and glutamatergic cells in the magnocellular layers (Fig. 3d–f). Furthermore, we report the same pattern of expression for FAAH and NAPE-PLD in both GABAergic (Fig. 3g–i and m–o) and glutamatergic neurons (Fig. 3j–l and p–r) without any preferences for any of them.

DISCUSSION

To our knowledge, this is the first study reporting the spatial distribution of CB1R and the enzymes regulating the levels of its ligands, namely FAAH and NAPE-PLD in the dLGN of primates. Given that CB1R, FAAH and NAPE-PLD are expressed in an overlapping pattern in the dLGN (Fig. 1), it might play a role in the auto-feedback control of neurotransmitter release, as proposed for the retina of the same species (Bouskila et al., 2012). This means that the same neurons that produce eCBs may also respond to their ligands in order to control the release of neurotransmitters.

CB1R: from the retina to the dLGN

There are studies that assessed CB1R expression in the whole brain and reported its expression in the thalamus. The dorsal thalamus was found to slightly express CB1Rs in rats (Tsou et al., 1998), not at all (Eggan and Lewis, 2007) or moderately (Ong and Mackie, 1999) in primates and humans (Glass et al., 1997), without any focus on the dLGN. To date, we have found only one study looking specifically at the rodent dLGN and reporting CB1R expression (Argaw et al., 2011). These results are however difficult to generalize to the monkey and human dLGN given the major anatomical differences in its organization as well as its cortical projections. Moreover, while the vast majority of retinal inputs projects to the dLGN in primates, only a limited number of retinal ganglion cells axons converge to the basic dLGN of rodents (Dacey et al., 2003; Huberman and Niell, 2011).

Retinal ganglion cells receive their input from rods and cones and transfer the visual information via parasol and midget cells to the magnocellular layers and the parvocellular layers of dLGN, respectively. Magnocellular and parvocellular layers target layer four of area V1 (4Cα and 4Cβ respectively). Both the M and P pathways also project to layer six of the primary visual cortex and receive a robust corticogeniculate feedback from the same layer that is mainly excitatory and glutamatergic (McCormick and von Krosigk, 1992; Fitzpatrick et al., 1994). The LGN is not just a passive relay; about 90% of its inputs are coming from sites other than retina, and about 30% of them are feedback inputs from V1 (Van Horn et al., 2000). Recent studies revealed that a close relationship in feedforward and feedback parallel streams instigates the functional influence of the LGN in visual processing. The magnocellular pathway is more sensitive to low spatial frequencies, low luminance contrasts, and responsible for the perception of motion and luminance, but it is chromatically non-opponent. On the other hand, parvocellular neurons (eight times more numerous than magno cells) convey chromatic and form information and are less sensitive to luminance contrasts (Briggs and Usrey, 2011). Additionally, the middle temporal visual area (MT) and medial superior temporal area (MST), motion detection centers, mainly receive the magnocellular layers' primary inputs (Maunsell et al., 1990; Merigan et al., 1991). In human and non-human primates, low to moderate density of CB1R has been reported in several cortical areas like the primary visual cortex (V1), specially layer five and six, in higher-order visual areas (V2, V3, V4) with more density in MT and MST (Eggan and Lewis, 2007). In V1, layers five and six contained the highest expression of CB1R (Eggan and Lewis, 2007). Interestingly, the higher density of CB1R in magnocellular layers of LGN in our study concurs with well-defined thalamo-recipient cortical areas. Thus, expression of eCB components in the visual cortex of rodent and primate brains (Eggan and Lewis, 2007; Jiang et al., 2010) indicates that the whole visual pathway, from the retina to cortex, can be influenced by cannabinoids.

CB1R and FAAH are highly co-expressed throughout the retinal layers of the same species (Bouskila et al., 2012). Here, we show that both CB1R and FAAH are present in the dLGN mainly in the magnocellular layers. Previous studies showed a similar overlapping distribution of FAAH and CB1R in pyramidal cells of the mouse hippocampus, amygdala and entorhinal cortex (Marsicano and Lutz, 1999) and the rat cortex (Hill et al., 2007).

NAPE-PLD: a dissimilar pattern of expression

NAPE-PLD is widely expressed in the mouse thalamus (Egertová et al., 2008). Furthermore, the presence of NAPE-PLD in the rat brain has been reported, with an increased expression in the thalamus (Morishita et al., 2005). Unlike CB1R and FAAH, the synthesizing enzyme, NAPE-PLD, is expressed homogenously throughout the magnocellular and parvocellular layers of the dLGN without any laminar preference (Fig. 1c, f, g). Besides synthesizing the endocannabinoid AEA, NAPE-PLD also generates NAEs that are major substrates for mediating various motivational functions (Viveros et al., 2008). Interestingly, the degrading enzyme FAAH can metabolize NAEs into cellular membrane components (Cravatt et al., 1996, 2001). Even though both FAAH and NAPE-

PLD are expressed in rodent thalamic nuclei neuronal cells, FAAH is only present in neuronal somata (Egertová et al., 2003). Given that these proteins are targeted to the axons, axon terminals and cytosol of neurons suggest a putative role of the eCB system as a mediator of anterograde signaling at thalamic synapses. Our results show that FAAH and NAPE-PLD are also co-expressed in the monkey dLGN (Fig. 1b, c). They support previously reported results that NAE could serve as an autocrine synaptic signaling molecules regulating the release of neurotransmitters (Egertová et al., 2008).

CB1R, FAAH and NAPE-PLD are not present in LGN astrocytes

The presence of CB1R in astrocytes is controversial. While some studies have failed to show any expression of CB1R in astrocytes (reviewed in Stella, 2004), others have detected it in the caudate, putamen (Rodriguez et al., 2001) and hippocampal astrocytes (Navarrete and Araque, 2008). In the hippocampus, astrocyte activation of CB1R leads to phospholipase C-dependent Ca^{2+} mobilization from the store and mediation of the eCBs communication with the neurons. This intermediation might play a role in the physiology of CB addiction (Navarrete and Araque, 2008). Our results show no co-expression between CB1R, FAAH and NAPE-PLD with GFAP in the LGN.

Functional significance

The geniculo-cortical distribution of CB1R (Fig. 1) sheds light into the putative functions of the eCB system in vision. Indeed, cannabis at the retinal level could affect the upstream visual pathways namely the ventral and dorsal visual streams. The higher expression of CB1R and FAAH in the magnocellular layers could have a functional value for the dorsal visual system involved in motion processing and object location (‘‘how/where’’ pathway) (Goodale and Milner, 1992; Kupers and Ptito, 2014). The abundance of the CB1R in the magnocellular layers of dLGN, areas MT and MST supports a role of eCB system in motion perception. In agreement with our findings, case studies on high-potency heavy cannabis smokers reported visual disturbances and impairment in motion perception (Levi and Miller, 1990). Likewise, cannabis causes impaired performance in tests that require fine psychomotor control such as tracking a moving point of light on a screen (Adams et al., 1975, 1978). Magnocellular neurons are also more sensitive to low luminance contrasts (Tootell et al., 1988) and relatively unresponsive to chromatic contrasts (Croner and Kaplan, 1995). Higher expression of CB1R in the magnocellular pathway prompts a role of the endocannabinoid system in the night vision. In agreement with this speculation, numerous reports claim that smoking marijuana improves dim light vision and photosensitivity (Dawson et al., 1977; Merzouki and Mesa, 2002; Russo et al., 2004). Besides, the neurons in the magnocellular pathway are also sensitive to flickering stimuli (Lee et al., 1989) and lesions to the magnocellular layers of the dLGN can cause deficits in critical flicker fusion (Merigan and Maunsell, 1990) and flicker detection (Schiller et al., 1990).

Even though the expression of the CB1R and FAAH is more abundant in magnocellular layers, they are nonetheless present in the parvocellular layers of the dLGN. If the eCB system plays any role in color perception, it should be through chromatic properties of parvo cells and retinal cones. Both of these components of the visual system express CB1R. Conjointly, one of the most frequently reported effects of cannabis is more intense and brighter colors (Green et al., 2003; Lerner et al., 2011). Although the eCB system is considered as a good candidate for modulation of the dynamics of the cortical networks (Robbe et al., 2006), there are few electrophysiological studies on the role of cannabinoids in the visual system. Recently, it has been reported that the CB1R and CB2R full agonist, CP55940, decreases electroencephalogram and local field potential power in V1 and V2 in macaque monkeys (Ohiorhenuan et al., 2014). To the best of our knowledge, there is only one study that has characterized the physiological effects of CB1R-mediated activity in the rat visual thalamus (Dasilva et al., 2012). Using single-unit extracellular recordings, the authors showed that, at the level of thalamus, CB1R activation revealed two cellular populations, one exhibiting excitatory effects (28%) and the other inhibitory ones (72%). These actions were blocked using AM251, a specific inverse agonist of CB1R. This suggests that CB1R in the rat thalamus acts as a dynamic modulator of visual information funneled to the cortex. The modulatory role of CB1R in the thalamus of monkeys and especially the dLGN could have a higher impact on visual processing due to its complex laminar structure and increased retinal inputs. Our results are in accordance with these electrophysiological findings and revealed that this neuromodulation of CB1R receptors may be due to their expression in the dLGN.

The expression pattern of these eCB components has been also well characterized in the primate retinal cells (Bouskila et al., 2012; Bouskila et al., 2013a,b) that project to the dLGN through the optic nerve. The importance of CB1R has been highlighted in a recent electroretinographic study (ERG) that showed the implication of this cannabinoid receptor in the generation of the ERG responses (Ptito et al., 2014). Indeed, blocking CB1R induces an increase in the b-wave component of the ERG. This increase is possibly reflecting the gating of calcium (Ca^{2+}) and potassium (K^{+}) ionic channels (Bouskila et al., 2013a). The change in neuronal membrane permeability to Ca^{2+} ions and activity of adenylyl cyclase may affect neurotransmitter release and action (Di Marzo et al., 1998) not only at the retinal level, but also probably at the dLGN level.

The data presented here provide the first insight into the neuroanatomy of CB1R, FAAH, and NAPE-PLD expression in the primate dLGN and a new perspective of the neural function of this system. In other words, the presence of the endocannabinoid system in the dLGN and especially in the magnocellular pathway suggests a putative neuromodulatory action that affects the functions of the dorsal visual pathway involved in motion

perception, object localization and action-oriented behaviors that depend on the perception of space.

CONFLICT OF INTEREST

The authors declare that they have no conflict of interest.

Acknowledgments—The Natural Science and Engineering Research Council of Canada (6362-2012, MP; 311892-2010, JFB) and the Canadian Institutes of Health Research (MOP-86495, JFB) supported this project financially. J.F.B. holds a Chercheur Boursier Senior from the Fonds de Recherche du Québec-Santé (FRQ-S). M.P is Harland Sanders Char Professor in Visual Science. We are also grateful to Dr. Frank Ervin and Dr. Roberta Palmour of St.-Kitts, West Indies, for supplying the vervet monkey tissues. We would like to thank Dr. Mohammad Jabbari Hagh for writing the MATLAB codes for heat map.

REFERENCES

Adams AJ, Brown B (1975) Alcohol prolongs time course of glare recovery. Nature 257(5526):481–483.

Adams AJ, Brown B, Flom MC, Jones RT, Jampolsky A (1975) Alcohol and marijuana effects on static visual acuity. Am J Optom Physiol Opt 52(11):729–735.

Adams AJ, Brown B, Haegerstrom-Portnoy G, Flom MC, Jones RT (1978) Marijuana, alcohol, and combined drug effects on the time course of glare recovery. Psychopharmacology (Berl) 56(1):81–86.

Argaw A, Duff G, Zabouri N, Cecyre B, Chaine N, Cherif H, Tea N, Lutz B, Ptito M, Bouchard JF (2011) Concerted action of CB1 cannabinoid receptor and deleted in colorectal cancer in axon guidance. J Neurosci 31(4):1489–1499.

Bouskila J, Burke MW, Zabouri N, Casanova C, Ptito M, Bouchard JF (2012) Expression and localization of the cannabinoid receptor type 1 and the enzyme fatty acid amide hydrolase in the retina of vervet monkeys. Neuroscience 202:117–130.

Bouskila J, Javadi P, Casanova C, Ptito M, Bouchard JF (2013a) Muller cells express the cannabinoid CB2 receptor in the vervet monkey retina. J Comp Neurol 521:2399–2415.

Bouskila J, Javadi P, Casanova C, Ptito M, Bouchard JF (2013b) Rod photoreceptors express GPR55 in the adult vervet monkey retina. PLoS One 8(11):e81080.

Breivogel CS, Sim LJ, Childers SR (1997) Regional differences in cannabinoid receptor/G-protein coupling in rat brain. J Pharmacol Exp Ther 282(3):1632–1642.

Briggs F, Usrey WM (2011) Corticogeniculate feedback and visual processing in the primate. J Physiol 589(Pt. 1):33–40.

Cravatt BF, Demarest K, Patricelli MP, Bracey MH, Giang DK, Martin BR, Lichtman AH (2001) Supersensitivity to anandamide and enhanced endogenous cannabinoid signaling in mice lacking fatty acid amide hydrolase. Proc Natl Acad Sci U S A 98(16):9371–9376.

Cravatt BF, Giang DK, Mayfield SP, Boger DL, Lerner RA, Gilula NB (1996) Molecular characterization of an enzyme that degrades neuromodulatory fatty-acid amides. Nature 384(6604):83–87.

Croner LJ, Kaplan E (1995) Receptive fields of P and M ganglion cells across the primate retina. Vision Res 35(1):7–24.

Dacey DM, Peterson BB, Robinson FR, Gamlin PD (2003) Fireworks in the primate retina: in vitro photodynamics reveals diverse LGN-projecting ganglion cell types. Neuron 37(1):15–27.

Dasilva MA, Grieve KL, Cudeiro J, Rivadulla C (2012) Endocannabinoid CB1 receptors modulate visual output from the thalamus. Psychopharmacology (Berl) 219(3):835–845.

Dawson WW, Jimenez-Antillon CF, Perez JM, Zeskind JA (1977) Marijuana and vision–after ten years' use in Costa Rica. Invest Ophthalmol Vis Sci 16(8):689–699.

Deutsch DG, Chin SA (1993) Enzymatic synthesis and degradation of anandamide, a cannabinoid receptor agonist. Biochem Pharmacol 46(5):791–796.

Di Marzo V, Melck D, Bisogno T, De Petrocellis L (1998) Endocannabinoids: endogenous cannabinoid receptor ligands with neuromodulatory action. Trends Neurosci 21(12):521–528.

Egertová M, Cravatt BF, Elphick MR (2003) Comparative analysis of fatty acid amide hydrolase and cb(1) cannabinoid receptor expression in the mouse brain: evidence of a widespread role for fatty acid amide hydrolase in regulation of endocannabinoid signaling. Neuroscience 119(2):481–496.

Egertová M, Elphick MR (2000) Localisation of cannabinoid receptors in the rat brain using antibodies to the intracellular C-terminal tail of CB. J Comp Neurol 422(2):159–171.

Egertová M, Giang DK, Cravatt BF, Elphick MR (1998) A new perspective on cannabinoid signalling: complementary localization of fatty acid amide hydrolase and the CB1 receptor in rat brain. Proc Biol Sci 265(1410):2081–2085.

Egertová M, Simon GM, Cravatt BF, Elphick MR (2008) Localization of N-acyl phosphatidylethanolamine phospholipase D (NAPE-PLD) expression in mouse brain: A new perspective on N-acylethanolamines as neural signaling molecules. J Comp Neurol 506(4):604–615.

Eggan SM, Lewis DA (2007) Immunocytochemical distribution of the cannabinoid CB1 receptor in the primate neocortex: a regional and laminar analysis. Cereb Cortex 17(1):175–191.

Emrich HM, Weber MM, Wendl A, Zihl J, von Meyer L, Hanisch W (1991) Reduced binocular depth inversion as an indicator of cannabis-induced censorship impairment. Pharmacol Biochem Behav 40(3):689–690.

Felder CC, Nielsen A, Briley EM, Palkovits M, Priller J, Axelrod J, Nguyen DN, Richardson JM, Riggin RM, Koppel GA, Paul SM, Becker GW (1996) Isolation and measurement of the endogenous cannabinoid receptor agonist, anandamide, in brain and peripheral tissues of human and rat. FEBS Lett 393(2–3):231–235.

Fitzpatrick D, Usrey WM, Schofield BR, Einstein G (1994) The sublaminar organization of corticogeniculate neurons in layer 6 of macaque striate cortex. Vis Neurosci 11(2):307–315.

Flom MC, Brown B, Adams AJ, Jones RT (1976) Alcohol and marijuana effects on ocular tracking. Am J Optom Physiol Opt 53(12):764–773.

Glass M, Dragunow M, Faull RL (1997) Cannabinoid receptors in the human brain: a detailed anatomical and quantitative autoradiographic study in the fetal, neonatal and adult human brain. Neuroscience 77(2):299–318.

Gómez-Ruiz M, Hernández M, de Miguel R, Ramos JA (2007) An overview on the biochemistry of the cannabinoid system. Mol Neurobiol 36(1):3–14.

Goodale MA, Milner AD (1992) Separate visual pathways for perception and action. Trends Neurosci 15(1):20–25.

Green B, Kavanagh D, Young R (2003) Being stoned: a review of self-reported cannabis effects. Drug Alcohol Rev 22(4):453–460.

Herkenham M, Lynn AB, Johnson MR, Melvin LS, de Costa BR, Rice KC (1991) Characterization and localization of cannabinoid receptors in rat brain: a quantitative in vitro autoradiographic study. J Neurosci 11(2):563–583.

Hill EL, Gallopin T, Ferezou I, Cauli B, Rossier J, Schweitzer P, Lambolez B (2007) Functional CB1 receptors are broadly expressed in neocortical GABAergic and glutamatergic neurons. J Neurophysiol 97(4):2580–2589.

Huberman AD, Niell CM (2011) What can mice tell us about how vision works? Trends Neurosci 34(9):464–473.

Jiang B, Sohya K, Sarihi A, Yanagawa Y, Tsumoto T (2010) Laminar-specific maturation of GABAergic transmission and susceptibility to visual deprivation are related to endocannabinoid sensitivity in mouse visual cortex. J Neurosci 30(42):14261–14272.

Jongen-Relo AL, Pitkanen A, Amaral DG (1999) Distribution of GABAergic cells and fibers in the hippocampal formation of the macaque monkey: an immunohistochemical and in situ hybridization study. J Comp Neurol 408(2):237–271.

Kupers R, Ptito M (2014) Compensatory plasticity and cross-modal reorganization following early visual deprivation. Neurosci Biobehav Rev 7634:191–197.
Lee BB, Martin PR, Valberg A (1989) Sensitivity of macaque retinal ganglion cells to chromatic and luminance flicker. J Physiol 414:223–243.
Lerner AG, Goodman C, Rudinski D, Bleich A (2011) Benign and time-limited visual disturbances (flashbacks) in recent abstinent high-potency heavy cannabis smokers: a case series study. Isr J Psychiatry Relat Sci 48(1):25–29.
Levi L, Miller NR (1990) Visual illusions associated with previous drug abuse. J Clin Neuroophthalmol 10(2):103–110.
Leweke FM, Schneider U, Thies M, Munte TF, Emrich HM (1999) Effects of synthetic delta9-tetrahydrocannabinol on binocular depth inversion of natural and artificial objects in man. Psychopharmacology (Berl) 142(3):230–235.
Marsicano G, Lutz B (1999) Expression of the cannabinoid receptor CB1 in distinct neuronal subpopulations in the adult mouse forebrain. Eur J Neurosci 11(12):4213–4225.
Maunsell JH, Nealey TA, DePriest DD (1990) Magnocellular and parvocellular contributions to responses in the middle temporal visual area (MT) of the macaque monkey. J Neurosci 10(10):3323–3334.
McCormick DA, von Krosigk M (1992) Corticothalamic activation modulates thalamic firing through glutamate ''metabotropic'' receptors. Proc Natl Acad Sci U S A 89(7):2774–2778.
Merigan WH, Byrne CE, Maunsell JH (1991) Does primate motion perception depend on the magnocellular pathway? J Neurosci 11(11):3422–3429.
Merigan WH, Maunsell JH (1990) Macaque vision after magnocellular lateral geniculate lesions. Vis Neurosci 5(4):347–352.
Merzouki A, Mesa JM (2002) Concerning kif, a Cannabis sativa L. preparation smoked in the Rif mountains of northern Morocco. J Ethnopharmacol 81(3):403–406.
Moldrich G, Wenger T (2000) Localization of the CB1 cannabinoid receptor in the rat brain. An immunohistochemical study. Peptides 21(11):1735–1742.
Morishita J, Okamoto Y, Tsuboi K, Ueno M, Sakamoto H, Maekawa N, Ueda N (2005) Regional distribution and age-dependent expression of N-acylphosphatidylethanolamine-hydrolyzing phospholipase D in rat brain. J Neurochem 94(3):753–762.
Moskowitz H, Sharma S, McGlothlin W (1972) Effect of marihuana upon peripheral vision as a function of the information processing demands in central vision. Percept Mot Skills 35(3):875–882.
Navarrete M, Araque A (2008) Endocannabinoids mediate neuron-astrocyte communication. Neuron 57(6):883–893.
Ohiorhenuan IE, Mechler F, Purpura KP, Schmid AM, Hu Q, Victor JD (2014) Cannabinoid neuromodulation in the adult early visual cortex. PLoS One 9(2):e87362.
Ong WY, Mackie K (1999) A light and electron microscopic study of the CB1 cannabinoid receptor in primate brain. Neuroscience 92(4):1177–1191.
Piomelli D (2003) The molecular logic of endocannabinoid signalling. Nat Rev Neurosci 4(11):873–884.
Ptito M, Javadi, P, Bouskila J, Casanova C, Bouchard JF. Role of retinal cannabinoid receptors CB1 and CB2, and GPR55 defined by electroretinography in vervet monkeys. FENS-0297-D021; 2014.
Robbe D, Montgomery SM, Thome A, Rueda-Orozco PE, McNaughton BL, Buzsaki G (2006) Cannabinoids reveal importance of spike timing coordination in hippocampal function. Nat Neurosci 9(12):1526–1533.
Rodriguez JJ, Mackie K, Pickel VM (2001) Ultrastructural localization of the CB1 cannabinoid receptor in mu-opioid receptor patches of the rat Caudate putamen nucleus. J Neurosci 21(3):823–833.
Russo EB, Merzouki A, Mesa JM, Frey KA, Bach PJ (2004) Cannabis improves night vision: a case study of dark adaptometry and scotopic sensitivity in kif smokers of the Rif mountains of northern Morocco. J Ethnopharmacol 93(1):99–104.
Schiller PH, Logothetis NK, Charles ER (1990) Role of the color-opponent and broad-band channels in vision. Vis Neurosci 5(4):321–346.
Semple DM, Ramsden F, McIntosh AM (2003) Reduced binocular depth inversion in regular cannabis users. Pharmacol Biochem Behav 75(4):789–793.
Stella N (2004) Cannabinoid signaling in glial cells. Glia 48(4):267–277.
Straiker A, Stella N, Piomelli D, Mackie K, Karten HJ, Maguire G (1999a) Cannabinoid CB1 receptors and ligands in vertebrate retina: localization and function of an endogenous signaling system. Proc Natl Acad Sci U S A 96(25):14565–14570.
Straiker AJ, Maguire G, Mackie K, Lindsey J (1999b) Localization of cannabinoid CB1 receptors in the human anterior eye and retina. Invest Ophthalmol Vis Sci 40(10):2442–2448.
Suárez J, Bermudez-Silva FJ, Mackie K, Ledent C, Zimmer A, Cravatt BF, de Fonseca FR (2008) Immunohistochemical description of the endogenous cannabinoid system in the rat cerebellum and functionally related nuclei. J Comp Neurol 509(4):400–421.
Takahata T, Hashikawa T, Tochitani S, Tochitani T (2010) Differential expression patterns of OCC1-related, extracellular matrix proteins in the lateral geniculate nucleus of macaque monkeys. J Chem Neuroanat 40(2):112–122.
Tootell RB, Hamilton SL, Switkes E (1988) Functional anatomy of macaque striate cortex. IV. Contrast and magno-parvo streams. J Neurosci 8(5):1594–1609.
Tsou K, Brown S, Sanudo-Pena MC, Mackie K, Walker JM (1998) Immunohistochemical distribution of cannabinoid CB1 receptors in the rat central nervous system. Neuroscience 83(2):393–411.
Van Horn SC, Erisir A, Sherman SM (2000) Relative distribution of synapses in the A-laminae of the lateral geniculate nucleus of the cat. J Comp Neurol 416(4):509–520.
Viveros MP, de Fonseca FR, Bermudez-Silva FJ, McPartland JM (2008) Critical role of the endocannabinoid system in the regulation of food intake and energy metabolism, with phylogenetic, developmental, and pathophysiological implications. Endocr Metab Immune Disord Drug Targets 8(3):220–230.
Wojcik SM, Rhee JS, Herzog E, Sigler A, Jahn R, Takamori S, Brose N, Rosenmund C (2004) An essential role for vesicular glutamate transporter 1 (VGLUT1) in postnatal development and control of quantal size. Proc Natl Acad Sci U S A 101(18):7158–7163.
Xu X, Ichida JM, Allison JD, Boyd JD, Bonds AB, Casagrande VA (2001) A comparison of koniocellular, magnocellular and parvocellular receptive field properties in the lateral geniculate nucleus of the owl monkey (*Aotus trivirgatus*). J Physiol 531(Pt. 1):203–218.
Zabouri N, Bouchard JF, Casanova C (2011) Cannabinoid receptor type 1 expression during postnatal development of the rat retina. J Comp Neurol 519(7):1258–1280.
Zhou J, Nannapaneni N, Shore S (2007) Vessicular glutamate transporters 1 and 2 are differentially associated with auditory nerve and spinal trigeminal inputs to the cochlear nucleus. J Comp Neurol 500(4):777–787.

(Accepted 13 December 2014)
(Available online 6 January 2015)